Journal of Materials and Environmental Science
ISSN: 2028-2508
e-ISSN: 2737-890X
CODEN: JMESCN

J. Mater. Environ. Sci., 2025, Volume 16, Issue 4, Page 591-601

http://www.jmaterenvironsci.com

Effect of Welding Parameters on Mechanical and Microstructure Behaviours of Welded Joints in Low-Carbon Steels for Engineering Applications

R. E. Njoku[1], I.Y. Suleiman[1, 2, 3]*, O. C. Ogheneme[6], K. Mu'azu[5], M. Z. Sirajo[4], E. V. Sochima[7], R. A. Raheem[3], O. Akponah[6], A. Omoraka[6], E. O. Amhenrior[6], M. T. Ijeamiran[6], K. C. Amamchukwu[1]

[1]Department of Metallurgical and Materials Engineering, University of Nigeria, Nsukka, Nigeria.
[2]African Centre of Excellence for Sustainable Power and Energy Development (ACE-SPED) University of Nigeria, Nsukka
[3]Department of Metallurgical and Materials Engineering, Federal University Lokoja, Nigeria
[4]Petroleum Technology Development Fund, Abuja, F. C. T., Nigeria
[5]Department of Pilot Plant and Fabrication, National Research Institute for Chemical Technology, Zaria, Nigeria.
[6]Department of Mechanical Engineering, Federal Polytechnic Orogun, Delta State, Nigeria.
[7]Department of Mechatronics Engineering, University of Nigeria, Nsukka, Nigeria

**Corresponding author, Email address: onoruoizadanjumas@yahoo.co.uk*

Received *06 Feb 2025,*
Revised *24 Mar 2025,*
Accepted *25 Mar 2025*

Keywords:
- ✓ *Welding parameters*
- ✓ *Low carbon steel,*
- ✓ *Mechanical properties,*
- ✓ *Welding current,*
- ✓ *Welding position.*

Citation*: Njoku R. E., Suleiman I. Y., Ogheneme O. C., Mu'azu K., Sirajo M. Z., Sochima E. V., Raheem R. A., Akponah O., Omoraka A., Amhenrior E. O., Ijeamira M. T., Amamchukwu K.C. (2025) Effect of Welding Parameters on Mechanical and Microstructure Behaviours of Welded Joints in Low-Carbon Steels for Engineering Applications. Mater. Environ. Sci., 16(4), 591-601.*

Abstract: The effect of welding parameters such as (welding current (WC), welding position (WP), electrode coating moisture content (MC), and electrode coating type (CT) were carried out on low-carbon steel. The microstructural changes and mechanical properties such as tensile strength, yield strength, and hardness in the weld zone under the influence of different welding parameters were also investigated. The welding current was varied from 100 A to 140 A at intervals of 20 A. Electrode coating type was varied between E6013 and E7018. The welding position was varied between flat and vertical up welding positions. Electrode coating moisture content was varied between oven-dried electrodes and damp electrodes. The results show that the electrode type superiority properties of E7018 can be traded off due to improper welding parameters. The sample welded with 120 amps displayed superior tensile and yield strengths to the other current settings. Those welded with the flat welding position displayed superior tensile and yield strength compared to those with the vertical up welding position. For the samples welded using different electrode coating moisture contents, it was deduced that the dry electrodes provided a weld with better mechanical properties than those made with the damp electrode. From the results, only a combination of the correct welding parameters for every chosen application would yield the desired mechanical and microstructure properties. The construction industry, **s**hipbuilding, and marine engineering such as hulls, decks, and other critical components***:***

1. Introduction

Over the years, mild steel has been used in many industrial applications and has received special preference due to its enormous properties such as strength, ductility, machinability, easy fabrication, and weldability (Abbas *et al.*, 2020). Of the many mild steel joining processes, Welding is a widely utilized process in engineering, especially for joining low-carbon steel components in various

applications, ranging from automotive and construction to shipbuilding and heavy machinery. Low-carbon steels are favoured in many engineering fields because of their high strength, ductility, and cost-effectiveness (Galvao *et al*, 2012; El Magri et al., 2025).

However, welding can significantly alter the mechanical and microstructural characteristics of welded joints, directly impacting the structures' performance, durability, and safety. The earliest instances of welding were carried out as forging processes as far back as 3000 BC (Guo *et al*, 2013). Since then, different methods of welding have been adopted for various industrial processes, and electric arc welding is the most preferred method of welding (Huang 2022).

This preference is due to its versatility, controllability, automation, and cost-effectiveness. The controllability of the process that takes centre place in the previous is evident in the ability of an operator to control the heat input and weld pool by adjusting parameters like current, voltage, and travel speed (Xiaoyi *et al*, 2019). To understand the effect of the change in parameters and resultantly carry out proper optimizations, one has to understand the effect of these welding parameters on the microstructure and mechanical properties of a weld.

The microstructure and mechanical properties of a weld go hand-in-hand because the mechanical properties of polycrystalline alloys and metals are greatly affected by their microstructures. An understanding of the microstructures of a weld gives an idea of the mechanical properties expected from it (Zhen *et al*., 2020).

The main focus of this research is to investigate the effect of welding parameters on the microstructure and mechanical properties of welded joints in low-carbon steel. The welded joints were created using the shielded metal arc welding process and some key parameters such as (welding current (WC), welding position (WP), electrode coating moisture content (MC), and electrode coating type (CT) were varied. The welding current was varied from 100A to 140 A at intervals of 20 A. Electrode coating type was varied between E6013 and E7018. The welding position was varied between flat and vertical up welding positions. Electrode coating moisture content was varied between oven-dried electrodes and damp electrodes. The effect of these variations on the microstructures and mechanical properties of the weld was then investigated.

2 Materials and Methods

2.1 Materials and equipment

The materials and equipment used in the course of this research work are as follows:
Mild steel plates of dimension 80mm x 40mm x 10mm, E6013 Mild steel electrodes, E7018 Low-hydrogen mild steel electrodes, cutting and grinding discs, hacksaw blades and frame, bench vice, angle grinder, wire brush, chipping hammer, welding helmet, Maxmech inverter welding machine, scriber, steel rule, grit papers (220, 320, 400, 800, 1200 grits), alumina powder, polishing pad, Optical microscope: Model MSC-M2000W, vital etchant, Testometric Universal Testing Machine, Rockwell Hardness Tester Model HRS-150.

2.2 Materials procurement

The metal samples and other metalworking materials were procured at the Metal Engineering Market in Ikorodu, Lagos. The chemicals used were sourced in Nsukka, Enugu State. A grinding spark test was carried out, and the chemical compositions were carried out using X-ray fluorescence (XRF) at Ajaokuta Steel Company, Kogi State Nigeria in line with the (Zakaria *et al*, 2010).

2.3 *Material preparation*

In this stage, the samples were cut from a full sheet to the dimensions of 40mm by 80mm, using an oxy-acetylene torch. A jig which was used to prevent the warping of the samples during welding was also cut out. The thickness of the samples and jigs was 10mm. After cutting, the samples were marked out to a 60-degree bevel and ground down using an angle grinder. The edges of the samples which were previously jarred due to the oxyacetylene cutting torch were also ground down.

A B

Figures 1a and 1b. Showing the materials used from cutting to welding

The suitable electrodes were also heated in an electrode oven to a temperature of 105°C for 30 minutes. This was done to eliminate any moisture that might have been picked up from the atmosphere and to satisfy the given process parameters for dry electrodes in the experiment. Another set of electrodes was exposed to steam for 15 minutes to simulate moisture absorption from the surroundings. **Figures 1a and b** show the materials from cutting to welding

2.4 Welding

The samples were fitted with a root gap of 2mm and tacked with the jigs to keep them in place. Each of the samples was welded with four passes. The first pass was the root pass and the last was the cap. The welding slag was chipped between each pass and the weld surface was cleaned with a wire brush before the commencement of another pass. This cleaning was to help remove any stuck slag that might contribute to inclusions or porosity in the weld. The suitable weld parameters were varied before the welding of each sample. For the sample that required vertical-up welding. The weld current was reduced to 90 amperes. This suitable amperage ensured that the weld metal did not sag during welding. **Table 1** illustrates all the parameters varied and the sample codes for each specimen which follows the findings (Vishnyakov *et al*, 2017).

2.5 Sample preparation for testing

In this stage, the samples were prepared for the tests to be carried out after the welding. The specimens for the tensile and impact tests were cut out of the bulk sample to a dimension of 5mm by the length of the final welded sample. The specimen for the microstructural analysis was cut from the centre of the welded sample to ensure that it comprised mainly of the weld metal (Ramesh *et al*, 2015). Each sample was properly identified to prevent any mix-ups during transportation or handling.

Table 1. Design of the experimental processes

Parameters	Variations	Sample codes
Electrode type (ET) (AWS specifications)	E6013	A1
	E7018	A2
Welding current (WC) (Amperes)	100	B1
	120	B2
	140	B3
Welding position (WP)	Flat	C1
	Vertical-up	C2
Electrode coating moisture content (MC)	Oven-dried electrodes	D1
	Damp electrodes	D2

A1-D2: The sample codes used during the duration of this research work

2.6 Grinding and Polishing

This step was carried out for the Optical microscopy and hardness samples. It involved three processes:
Rough grinding: This process involves filing the metal surface to even it out and remove any burns, scratches, and nicks from the weld cross-section. This is essential to ensure an even contact between the metal and grit paper during smooth grinding.
Smooth grinding: This process was carried out using grit papers of 220, 320, 400, 800, and 1200 grit as reported by (Jonathan *et al*, 2019**)**. It was done on a grinding pad with water as a lubricant.
Polishing: This process was carried out on a polishing disc with diamond paste powder, and a little bit of water. The specimens were cleaned and dried after this, in preparation for etching.
Etching: The specimens were etched by dipping their polished surfaces in a Nital etchant for 1 minute. Nital was used because the specimens were made of low-carbon steel and under (Khubaib *et al*, 2022).

2.7 Tensile test

The tensile test was carried out at the Nigerian Liquefied Natural Gas laboratory, Department of Metallurgical and Materials Engineering, University of Nigeria Nsukka using a Testometric Universal Testing Machine at room temperature. The test specimens were 100mm long with 10mm breadths and 5mm thickness. Each specimen was fitted to the jaws of the machine and secured tightly. The machine was then set using its attached computer to pull the specimens apart until they fractured. The test data was then uploaded to a compact disk for further analysis. The picture of the Testometric Universal Testing Machine is being presented in **Figure 2** was in accordance with work of (Bekir, 2018).

2.8 Microstructural Analysis

The microstructural analysis was done at the Metallurgical and Materials Engineering laboratory at the Enugu State University of Science and Technology Enugu State. The sample surfaces to be viewed were prepared in this laboratory. It was carried out using an Optical Microscope Model MSC-M2000W fitted with a Charged-Coupled Device (CCD) camera. Images of the microstructure were subsequently printed for further analysis (Aslanlar *et al.*, 2007).

2.9 Hardness testing

This test was carried out on the already prepared surface of the test specimens after microscopy analyses. This was also carried out at the Metallurgical and Materials Engineering Laboratory at the

Enugu State University of Science and Technology. The hardness testing machine used was a Rockwell hardness tester Model HRS-150 (Fermin *et al*, 2020).

Figure 2. Testometric Universal Testing Machine

3 Results and discussion

3.1 Mechanical properties

3.1.1 Ultimate Tensile Test Values

The ultimate tensile strength (UTS) of welded mild steel depends on the welding current and other factors such as electrode type, welding technique, and material properties. Typically, the welding current directly influences the weld quality, affecting the UTS values (Baghjari *et al.*, 2013). Figure 3 presents the results of the ultimate tensile strength against Sample codes. It has been established that low welding current can lead to insufficient heat input, cause incomplete fusion, poor penetration, and porosity, and result in low UTS values due to weak welds. However, in optimal welding current proper fusion and penetration can be achieved. It produces a strong and ductile weld, and results in high UTS values. Finally, a high welding current can lead to excessive heat input causing overheating, grain coarsening, and warping, which may lead to burn-through or slag inclusions and reduce the UTS due to weld defects (Aslanlar *et al.*, 2007).

The samples that exhibited the lowest tensile strength values are samples B1 and D2 welded with the damp electrode and 100 amps welding current respectively. This low welding current for B1 resulted in a low heat input which led to a rapid cooling of the weld metal and the heat-affected zone, thereby increasing the hardness of the surrounding base metal as stated observed by (Bekir, 2018). The low ultimate tensile strength values for D2 can be attributed to the weakness due to the hydrogen embrittlement in the weldment. Using damp electrodes during welding can have detrimental effects on the ultimate tensile strength (UTS) of mild steel due to increased hydrogen content, porosity formation, poor fusion and inclusions, oxidation, and reduced mechanical properties (Ramesh *et al*, 2015). From Figure 3, Sample A2, which was welded using the E7018 low hydrogen electrode, displayed a slightly lower tensile strength than samples A1, B2, B3, C1, C2, and D1, respectively.

Using **E7018 electrodes** for welding mild steel is supposed to have a positive impact on ultimate tensile strength (UTS) when the electrodes are properly handled and stored. This is because the electrodes are specifically designed for high-strength welds with excellent mechanical properties.
However, if E7018 electrodes are not properly stored or become damp, the UTS can be negatively affected due to hydrogen-induced cracking, porosity or inclusions, and reduced weld toughness (Huang 2022). Sample B3 was welded with a higher welding current of 140 amps, displaying a slightly lower tensile strength than the sample welded with a 120 amps welding current.

This behaviour is due to the ease of defect formation from the high heat input. These formed defects could affect the mechanical properties of the weld like tensile strength (Guo *et al.*, 2013). Samples A1, B2, C1, and D1 exhibit the highest values for tensile strengths during the analyses. These samples have the most ideal combinations of welding parameters for engineering applications.

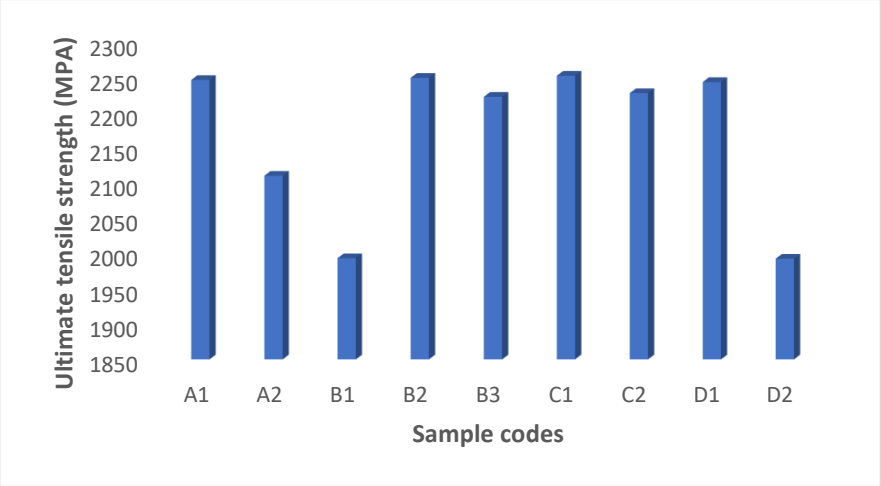

Figure 3. Variation of Ultimate Tensile strength against Sample codes

3.3.2 Yield Strength Values

Similar to the tensile strength values, the same set of samples A1, B2, C1, and D1 displayed the highest values for yield strengths. The sharp contrast between the values with the highest tensile strengths and those with the lowest which was very evident in the Ultimate tensile strength graph is not evident here. The yielding of all the samples occurred within an 80 MPa range. Sample C2 (Welded using the vertical-up procedure) displayed the lowest yield strength among the samples. This reduction in yield strength is due to the increased heat input due to the slow welding speeds used in the vertical-up welding procedure. In concurrence with the findings of (Huang 2022), higher heat input results in a reduction in the mechanical properties of the sample.

Sample B1 has a higher yield strength than C2 but a lower one than the other samples. This relatively low yield strength can also be attributed to the hardening caused by the low heat input (Xiaoyi *et al.*, 2019). The values of yield strength are presented in **Figure 4.**

3.3.3 Hardness values

Welding parameters affect the microstructural transformations in the weld and HAZ, influencing hardness values. Optimizing these parameters ensures a balance between adequate hardness for strength and toughness without excessive brittleness or softening. Proper control of heat input, cooling rates, and post-weld treatments is essential for achieving uniform and desirable hardness profiles in low-carbon steel welded joints (Abbas *et al*, 2020).

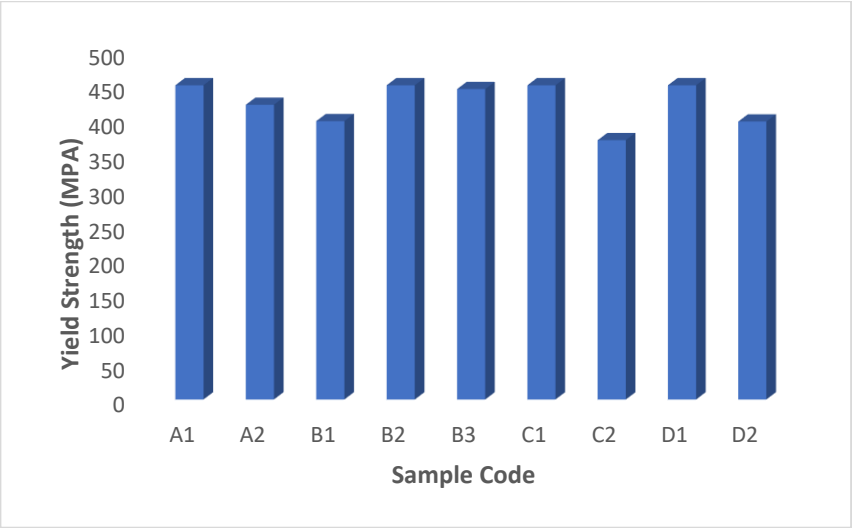

Figure 4. Variation of Yield strength against Sample codes

Figure 5 presents the results of the hardness for each of the samples. Unlike the ultimate tensile strength values which were not completely representative of each weld, the hardness values were obtained from the weld metal itself. Sample B3 (welded with 140 amps welding current) has the highest hardness value, while sample A2 has the lowest value. Since sample B3 has the second highest heat input among all the welds, its high hardness goes according to the research done by (Khubaib et *al*, 2022). It is believed that the high heat leads to an increase in the tendency for defect formation which in turn affects the hardness characteristic of the sample.

Sample B1 (Welded with 100 amps) which has the second highest hardness value can be attributed to the faster cooling rate due to the low heat input during welding. This fast-cooling rate resulted in the hardening of the weld.

Sample D2 (welded with a damp electrode) also has a high relative hardness which is due to the formation of defects in it such as hydrogen embrittlement [13]. The low hardness values of sample A2 (Welded with the E7018 electrode) can be attributed to its special electrode coating constituents which contain additives for crack prevention. Samples A1, B2, C1, and D1 have median hardness values which are similar to each other because they were welded using the same parameters and also confirmed to the previous findings of (Zhen *et al.*, 2020).

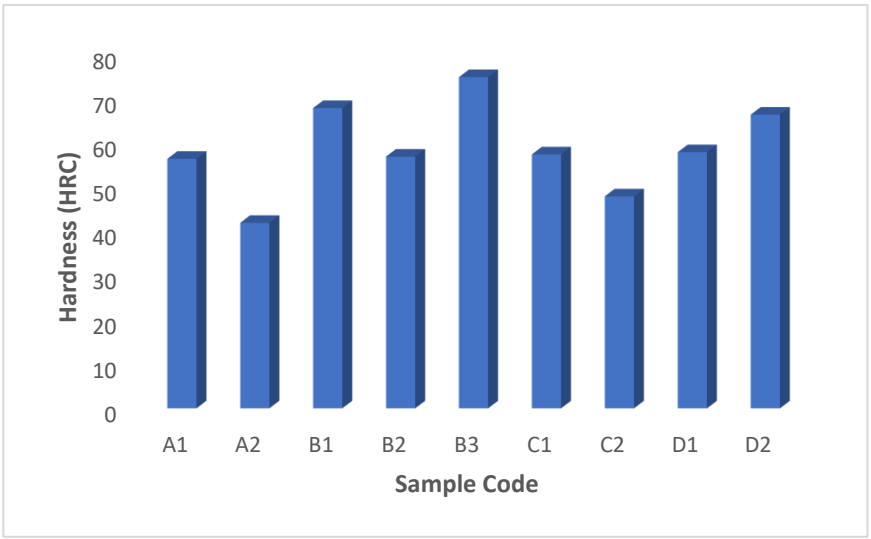

Figure 5. Variation of Hardness against Sample codes

The only sample that did not exhibit this phenomenon was sample D2. Sample D2 fractured directly from the weld joint. This sample was welded with an electrode dampened by exposing it to steam for 15 minutes. The reason for its deviation from the collective strengthening phenomenon exhibited by other samples can also be attributed to hydrogen embrittlement caused by hydrogen picked up from the moisture content of the electrode coating, due to the steam exposure (Xiaoyi *et al.*, 2019).

3.1 Microstructural analysis

Welding alters the microstructure of mild steel, particularly in the weld metal and HAZ, by introducing phase transformations and grain size variations. Proper control of welding parameters and post-weld treatments can optimize the microstructure, balancing hardness, strength, and toughness while minimizing defects such as brittle phases or excessive grain growth. As established earlier, microstructures of materials play an important role in the overall performance of engineering materials (Fermin *et al*, 2020). Samples A2, B2, C1, and D1 were welded using the same parameters, one image was used to represent their properties. All the microscopy images were taken at 100x magnification.

Figure 6a shows the microstructure of sample A2, it displayed the typical pearlite in a ferrite matrix structure which is a typical structure of low-carbon steels. There is also the presence of a different phase of unidentified welding products. These products could range from oxides, nitrides or silicates. They are responsible for the low hardness values on the sample, as they can inhibit grain growth in the metal during solidification. This effect might be intentional to produce a resulting "softening" effect on the weld which eliminates brittleness according to the findings of (Ramesh *et al,* 2015).

Figure 6b below is the microstructural image of sample B1, it presented a very fine arrangement of the pearlite in the ferrite matrix. This fine arrangement is attributed to the rapid cooling of the weld which resulted in a corresponding elevated hardness value evident in the Rockwell hardness value of the sample. There is also the presence of two inclusions at the bottom part of the image (Galvao *et al.*, 2012). **Figure 6c** below is an image of the microstructure of sample B2, there is an even distribution of the pearlite phases in the ferrite matrix. The grains are coarser than those of sample B1 which are more refined and there is a corresponding reduction in hardness in comparison to B1. This grain structure provided the sample with the ideal hardness value exhibited. The microstructure represents those of A1, C1, and D1 and is confirmed in the works of (Fermin *et al*, 2020).

Figure 6d below is an image of sample B3, it is evident that it has the most refined grain structure of all the samples. This very packed grain structure is the reason why it exhibited the highest hardness values among the samples. This structure resulted from the high heat input which gave room for defect formation in the weld and agreed to the findings of (Huang, 2022).

Figure 6e presents the image of sample C2, there is less refinement of the grain structure, and this contributed to its reduced hardness when compared to other samples apart from sample A2. Its microstructure also consists of coarse pearlite in a ferrite matrix (Khubai *et al*, 2022). Figure 6f shows the image of sample D2, it contained typical ferrite and pearlite structures observed in previous samples. It can also be observed that there are non-metallic phases that can be said to be hydrogen. These non-metallic phases caused the hydrogen embrittlement which made the tensile sample fracture from the weld (Aslanlar *et al*, 2007).

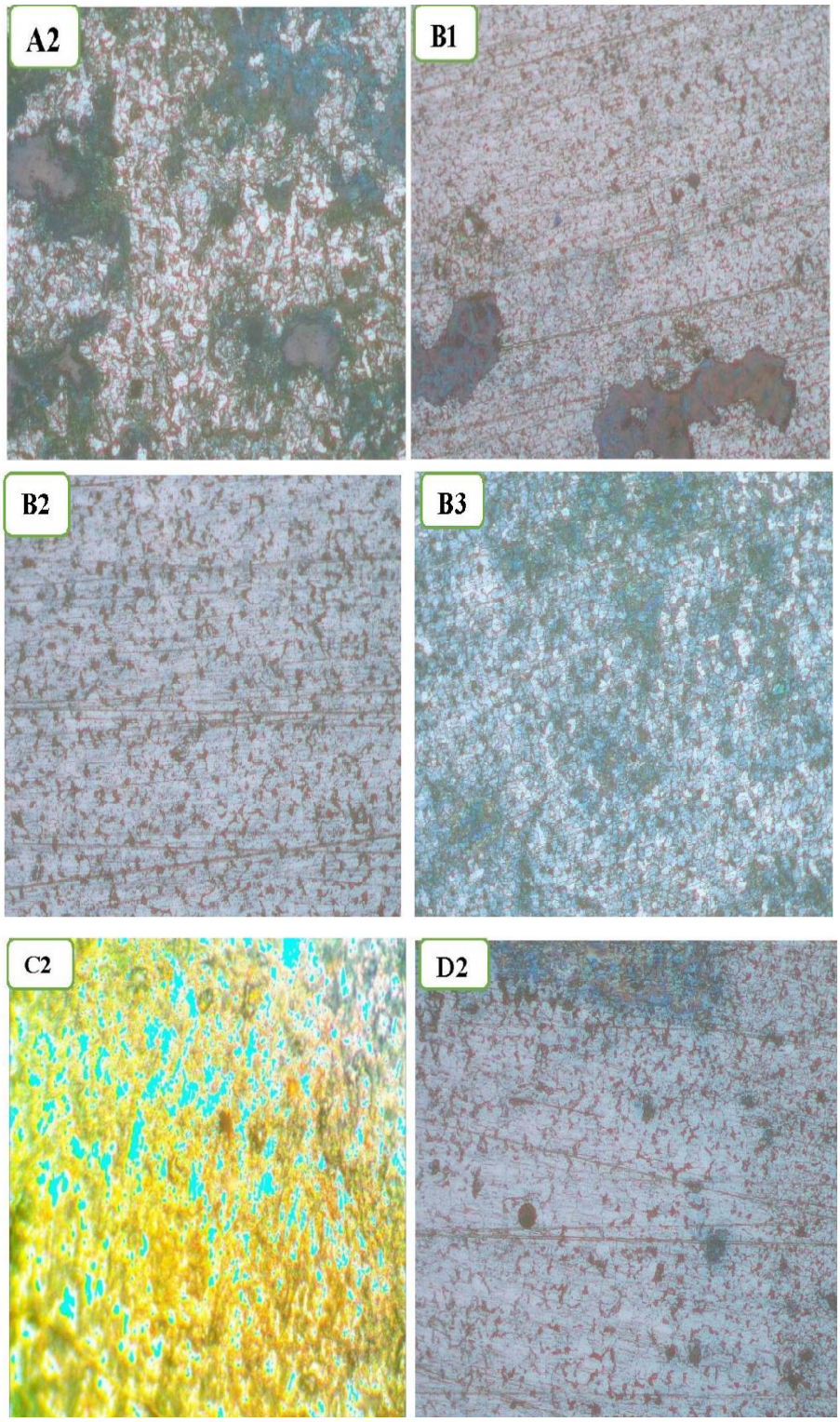

Figure 6. (a) Microstructural image of Sample (a) Sample A2. (b) Sample B1.(c) Sample B2. (d) Sample B3 (e) Sample C2, and (f) Sample D2

4 Conclusion

The following conclusions can be drawn from the results obtained:

1. Samples with the varied electrode coating types were observed that have superior properties reported for E7018 electrodes. However, these superior properties can be traded off due to improper welding parameters.

2. Samples with varied currents showed that only an optimal current can produce the most desired welding properties, and any upward or downward variation of this current would prove counterproductive to the endeavour.
3. The samples welded with 120 amps displayed superior tensile and yield strengths compared to the other current settings while samples welded with flat welding position displayed superior tensile and yield strength compared to the ones welded with the vertical up welding position.
4. Samples welded using dry electrodes provided a weld with better mechanical properties than those made with the damp electrode.
5. Proper control of welding parameters and post-weld treatments can optimize the microstructure, balancing hardness, strength, and toughness while minimizing defects such as brittle phases or excessive grain growth.

Acknowledgements: The authors are thankful to the staff of the Department of Metallurgical and Materials Engineering, University of Nigeria, Nsukka and Enugu State University of Science and Technology Enugu, Enugu State.

References

Abbas R, Mahmood K, Esmaeil H. (2020). Mechanical properties of steel welds at elevated temperatures. *J Constr Steel Res*.; 167, 105853. https:// doi. org/ 10. 1016/j. jcsr. 2019. 105853.

Aslanlar S, Ogur A, Ozsarac U, Illhan E, Demir Z. (2007). Effect of welding current on mechanical properties galvanised chromided steel sheets in electrical resistance spot welding. *Mater Des*. 28, 2–7. https:// doi. org/ 10. 1016/j. matdes. 2005. 06. 022.

Baghjari S. H, Akbari M.S.A.A. (2013). Effects of pulsed Nd: YAG laser welding parameters and subsequent post-weld heat treatment on microstructure and hardness of AISI 420 stainless steel. *Mater Des*. 43, 1–9. https:// doi. org/ 10. 1016/j. matdes. 2012. 06. 027.

Bekir C. (2018). Analysis of welding groove configurations on the strength of S275 structural steel welded by FCAW. *J Polytech*, 21, 489–95. https://doi. org/ 10. 2339/ polit eknik. 389642

El Magri, A., Hsissou, R., Ech-chihbi, E. *et al.* (2025). Exploring new formulated polymer composite coatings by glass for corrosion protection of additively manufactured 316 L stainless steel alloy in acidic environment: electrochemical measurements characterization and computational approaches. *Prog Addit Manuf* https://doi.org/10.1007/s40964-025-01024-5

Fermin B, Alejandro S, Moises B, Bartolome S, Jorge S. (2020). Surface quality and free energy evaluation of S275 steel by shot blasting, abrasive water jet texturing and laser surface texturing. *Metals*, 10, 1–19.

Galvao I, Oliveria J.C, Loureiro A, Rodrigues D.M. (2012) Formation and distribution of brittle structures in friction stir welding of aluminium and copper: influence of shoulder geometry. *Intermetallics*, 22(2012), 122–8. https:// doi. org/ 10. 1016/j. inter met. 2011. 10. 014.

Guo-Li L, Shan-Wu Y., Hui-Bin W, Xue-Li L (2013). Microstructures and mechanical performances of CGHAZ for oil tank steel during high heat input welding. *Rare Met*, 32, 129–33. https:// doi. org/ 10. 1007/ s12598- 013- 0036-y.

Huang N. (2022) Welding Speed and Current in Machine Human Cooperative Welding, *Crystals*, 12.113-120. https://doi.org/10.3390/cryst1202023

Jonathan G, Agustin G, Hernan S. (2019). Effect of welding parameters on nanostructured Fe-(C, B)-(Cr, Nb) alloys. *Mater Res*, 22, 1–8. https://doi. org/ 10. 1590/ 1980- 5373- MR- 2019- 0469.

Khubaib Z.G, Sadaqat A, Emad U.D, Aamir M, Niaz B.K, Syed W.A. (2022). Experimental investigation of welding parameters on surface roughness, microhardness, and tensile

strength of AISI 316L stainless steel welded joint using 308L filler material by TIG welding. *J Mater Res Technol*, 21, 220–36. https:// doi. org/ 10. 1016/j. jmrt. 2022. 09. 016.

Ramesh K.B, Chauhan N, Raole P.M, Harshad N. (2015). Studies on mechanical properties microstructure and fracture morphology details of laser beam welded thick SS304L plates for fusion reactor applications. *Fusion Eng Des*, 95, 34–43. https:// doi. org/ 10. 1016/j. fusengdes. 2015. 04. 001.

Vishnyakov V. I. Kiro S.A, Oprya M.V, Ennan A.A. (2017). Effects of shielding gas temperature and flow rate on the welding fume particle size distribution. *J Aerosol Sci*, 114, 55–61. https:// doi. org/ 10. 1016/j. jaero sci. 2017. 09. 010.

Xiaoyi H, Hui C, Zongtao Z, Chuang C, Chengzhu Z. (2019). ffect of shielding gas on welding process of laser-arc hybrid welding and MIG welding. *J Manuf Proces*, 38, 530–42. https:// doi. org/ 10. 1016/j. jmapro. 2019. 01. 045.

Zakaria B, Chemseddine D, Thierry B. (2010). Effect of welding on microstructure and mechanical properties of an industrial low carbon steel. *Engineering*, 2, 502–6. https:// doi. org/ 10. 4236/ eng. 2010. 27066.

Zhen M, Minghui Z, Muqin L. (2020). Effect of main arc voltage on arc behavior and droplet transfer in tri-arc twin wire welding. *J Market Res*, 9, 4876–83. https:// doi. org/ 10. 1016/j. jmrt. 2020. 03. 007.